IV International Conference on Particle-based Methods – Fundamentals and Applications
PARTICLES 2015
E. Oñate, M. Bischoff, D.R.J. Owen, P. Wriggers & T. Zohdi (Eds)

APPLICATION OF THE LATTICE BOLTZMANN METHOD IN ACOUSTICS

ERIK M. SALOMONS[1], WALTER J.A. LOHMAN[1], AND HAN ZHOU[1]

[1] TNO Netherlands Organization of Applied Scientific Research
Van Mourik Broekmanweg 6, 2628 XE Delft, The Netherlands
e-mail: erik.salomons@tno.nl

Key words: Lattice Boltzmann method, fluid flow, acoustics, porous materials.

Abstract. In this paper, practical aspects of the lattice Boltzmann method for fluid flow are explored and application to sound propagation is investigated. This work was performed within the framework of the European ITEA project MACH, which aims at optimizing scientific calculations on various parallel platforms. For fluid flow, our attention was drawn to the lattice Boltzmann method because of its advantages over other methods: the method is suitable for parallel computation, and it can be applied easily to systems with complex boundaries, such as porous media. We first developed simple 2D and 3D lattice Boltzmann codes for fluid flow in a lid-driven cavity. We explored possibilities to run it on the GPU of a personal computer, and we investigated GPU speedup factors. Next we developed a lattice Boltzmann code for simulation of sound waves. Various acoustic phenomena were investigated with this code, such as geometrical spreading of sound waves generated by a point source, reflection of sound waves by a rigid surface, and diffraction of sound waves by a noise barrier. Reflection of sound waves by a porous medium was also explored, and a comparison was made with theoretical solutions. Finally, the possibility to simulate sound propagation in an atmosphere with wind and temperature gradients was considered.

1 INTRODUCTION

Traditional methods for simulating fluid flow are based on the equations for conservation of mass and momentum in a fluid, i.e. the continuity equation and the Navier Stokes equations, respectively (see Refs. [1][2], for example). The conservation equations are differential equations based on the continuum model of a fluid. The equations can be solved by various numerical techniques.

The lattice Boltzmann method (LB method, or LBM) is an alternative approach for calculating fluid flow. An introduction to the LB method, and references to the literature, can be found in Ref. [3]. The LB method originates from lattice gas automata (LGA) for simulating fluid flow, which were developed in the 1980s. While the LGA method works with discrete particles on a regular lattice, the LB method works with a particle distribution function. The LB method is based on the Boltzmann equation from kinetic gas theory, which describes how distributions of particles in a gas propagate and collide [1]. Collisions may be modeled by the Bhatnagar-Gross-Krook (BGK) collision operator. The LB method with the BGK operator is often referred to as the LBGK method. From the LBGK equations, the Navier Stokes and continuity equations can be derived, under certain limiting conditions that depend on the actual formulation. Common limiting conditions are weak compressibility and

low Mach number (see Ref. [4] and references cited therein).

Sound propagation in the atmosphere is basically a special case of fluid flow. A sound wave is a small perturbation of the pressure and fluid velocity, which travels with the speed of sound. Consequently, fluid flow models may be applied for simulating sound propagation. An early application of the LB method to sound propagation is described in Ref. [5]. An extensive study of application of the LB method in acoustics was recently performed by Viggen [6][7].

In the present paper, application of the LB method in outdoor acoustics is described. A few practical cases are considered, including the cases of sound propagation near a (porous) ground surface and sound propagation over a noise barrier. A preliminary conclusion is that the LB method may be more powerful in dealing with complex geometries than other numerical methods in outdoor acoustics are [8][9][10][11].

This work was performed within the framework of the European ITEA project MACH, which aims at optimizing scientific calculations on various parallel platforms [12]. Computational fluid dynamics is one of the fields of application considered in MACH. We decided to explore the LB method because of its advantages over other fluid-flow simulation methods: the LB method is suitable for parallel computation, and it can be applied easily to systems with complex boundaries, such as porous media. Previous work on speeding up LB models by means of parallel computation, including computation on GPUs and supercomputers, is described in Refs. [13][14]. The focus in MACH is on (semi) automatic generation of computer code suitable for running on various platforms for parallel computation.

2 LATTICE BOLTZMANN METHOD FOR FLUID FLOW

2.1 Method

With the LB method a fluid is represented by means of a particle distribution function on a regular lattice [3]. The value of the distribution function at a lattice node represents the density of fluid particles at the node. Different particle velocities are distinguished, corresponding to the movement of particles to different neighboring lattice nodes during a time step. Consequently, the particle distribution function varies not only with position in the lattice but is also a function of the discrete set of particle velocities.

The LB particle distribution function is denoted as $f_i(\mathbf{x},t)$, where index i = 0, 1, 2, … distinguishes the different velocities to neighboring lattice nodes, $\mathbf{x}$ denotes position on the lattice, and t represents time. Here we consider the formulation of the LB method based on the BGK (Bhatnagar-Gross-Krook) approximation. The evolution of the fluid is represented by the following equation:

$$f_i(\mathbf{x}+\mathbf{e}_i\Delta t, t+\Delta t) = f_i(\mathbf{x},t) - \frac{1}{\tau}\left(f_i(\mathbf{x},t) - f_i^{\mathrm{eq}}(\mathbf{x},t)\right), \tag{1}$$

where $\mathbf{e}_i$ are the velocity vectors to neighboring nodes, Δt is the time step, τ is the relaxation time, and f_i^{eq} is the local equilibrium distribution function. We choose length and time units such that lattice spacing Δx and time step Δt are unity, so the particle speed $c = \Delta x/\Delta t$ is also

unity. The first part of the equation, $f_i(\mathbf{x}+\mathbf{e}_i\Delta t, t+\Delta t) = f_i(\mathbf{x},t)$, represents streaming of particles between neighboring nodes. The last term represents collisions between particles. Collisions of the fluid particles correspond to a relaxation towards local equilibrium.

Figure 1 illustrates the widely used D2Q9 lattice for the LB method in 2D. There are nine velocity vectors $\mathbf{e}_i$ to neighboring lattice nodes: $\mathbf{e}_0 = (0,0)$, $\mathbf{e}_1 = (1,0)$, $\mathbf{e}_2 = (0,1)$, …, $\mathbf{e}_8 = (1,-1)$. Here we have used an *xy* coordinate system with a horizontal *x* axis and a vertical *y* axis. The first vector $\mathbf{e}_0$ corresponds to zero velocity, so particles with $i = 0$ do not move to a neighboring node.

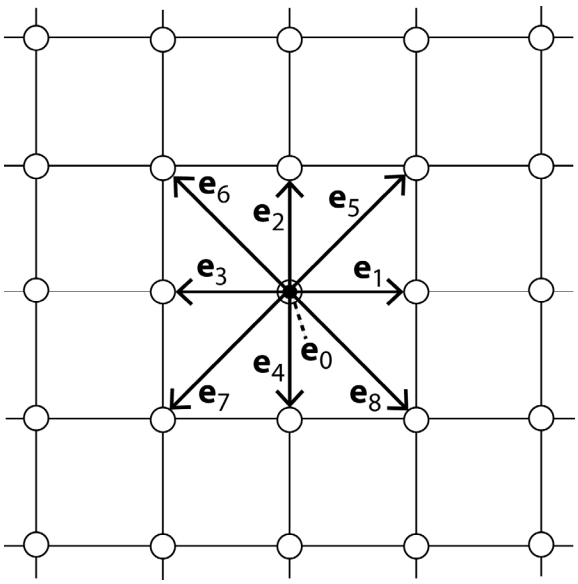

Figure 1: Rectangular 2D lattice illustrating the 2DQ9 scheme for the LB method.

The macroscopic fluid density ρ and the fluid velocity $\mathbf{u}$ follow from the distribution function: $\rho = \sum_i f_i$ and $\mathbf{u} = \frac{1}{\rho}\sum_i f_i\,\mathbf{e}_i$. The fluid density is related to the pressure *p* through the ideal gas law $p = c_s^2\rho$, where c_s is the sound speed in lattice units $\Delta x/\Delta t$, which is $1/\sqrt{3}$ for the D2Q9 and D3Q19 lattices. The density is included in the LB model as an independent variable in a regime close to fluid incompressibility [4]. The relaxation time τ is related to the kinematic shear viscosity ν of the fluid: $\nu = c_s^2\left(\tau - \frac{1}{2}\right)$. The viscosity is positive for $\tau > \frac{1}{2}$. As τ approaches $\frac{1}{2}$ numerical difficulties may occur. A safe choice is $\tau = 1$, which gives $\nu = \frac{1}{6}$. In the BGK approximation, the equilibrium distribution function is given by

$$f_i^{\mathrm{eq}} = w_i\rho\left(1 + \frac{\mathbf{e}_i\cdot\mathbf{u}}{c_s^2} + \frac{(\mathbf{e}_i\cdot\mathbf{u})^2}{2c_s^4} - \frac{\mathbf{u}^2}{2c_s^2}\right), \tag{2}$$

which is a truncated expansion of the Maxwell velocity distribution. The factors w_i are weight factors for the different velocity directions. For the D2Q9 scheme, the weights w_i are

$(\frac{4}{9},\frac{1}{9},\frac{1}{9},\frac{1}{9},\frac{1}{9},\frac{1}{36},\frac{1}{36},\frac{1}{36},\frac{1}{36})$ for $i = 0,1,\ldots,8$.

The core of a LB code is a loop over four elements:

- collisions
- streaming
- boundary conditions
- macroscopic quantities.

The first three elements yield updates of the distribution function, due to collisions, streaming, and boundary conditions, respectively. The fourth element is the calculation of density ρ and velocity components u and v of fluid velocity $\mathbf{u} = (u,v)$, which are used in the collision calculation.

Different types of boundary conditions exist. At a stationary boundary (zero velocity at a wall) one may apply bounceback conditions, which means that a distribution function component f_i directed into the fluid is obtained from the component in the opposite (outward) direction. First-order and second-order bounceback formulations have been developed [3]. For a boundary with an imposed velocity or pressure, boundary conditions were presented in Ref. [15].

2.2 Lid-driven cavity

Figure 2 shows results of a D2Q9 LB calculation for the case of a lid-driven cavity in 2D. The fluid is enclosed in a square box with solid walls, while at the top of the box a constant horizontal velocity u_0 is imposed as a boundary condition. The calculation was performed for a 1000x1000 grid, with $u_0 = 0.06$ and $\nu = 0.06$. The Reynolds number $\mathrm{Re} = u_0 L / \nu$ is equal to 1000 in this case, with grid size L=1000. The graphs show the (steady state) fluid flow after $16 \cdot 10^4$ time steps.

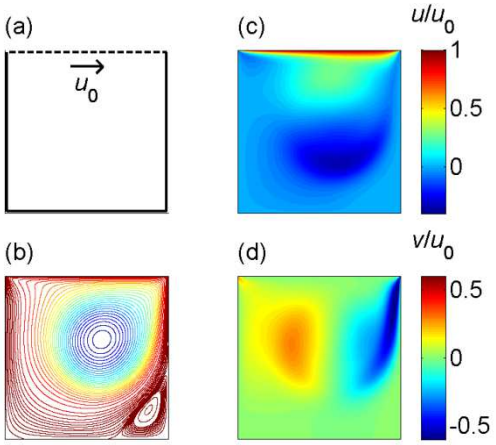

Figure 2: Results of a LB calculation for a lid-driven cavity, with the geometry (a), streamlines (b), and normalized velocity components u/u_0 (c) and v/u_0 (d).

2.3 Calculation times and GPU speedup

As mentioned in Section 1, this work was performed within the framework of the European project MACH, which aims at speeding up various types of scientific calculations. In this section we present a few calculation times for the LB model for a lid-driven cavity (see previous section). Calculations were performed with non-optimized codes on a PC with a 2.4 GHz CPU (Intel Xeon E5620, 6GB RAM) and an NVIDIA GPU (GeForce GTX 680, 4GB, 1536 CUDA cores).

For a 2DQ9 100x100 grid with Re=1000 ($u_0 = 0.6,\ \nu = 0.06$) we achieved a steady state within 4000 time steps, which took about 20 seconds with a Matlab code and 8 seconds with a code converted to C/C++ (running on a single CPU core). These times correspond to 2 and 5 MLUPS, respectively (MLUPS = mega lattice site updates per second). With a CUDA code [16] running on the GPU we found 2 seconds.

For a 2DQ9 1000x1000 grid with Re=1000 ($u_0 = 0.06,\ \nu = 0.06$) we needed $16 \cdot 10^4$ time steps to achieve a steady state, and with a Matlab code this took 32h (running on a single CPU core), corresponding to 1.4 MLUPS. With a modified Matlab code that employs the GPU, making use of the Matlab parallel processing toolbox, the time was 12h, corresponding to 3.7 MLUPS. The total number of $16 \cdot 10^4$ time steps is nearly two orders of magnitude larger than the 4000 times steps for the 100x100 grid, due to the fact that the equilibration time scales with the square of the linear grid size [17].

For a 3DQ19 100x100x100 grid with Re=1000 ($u_0 = 0.6,\ \nu = 0.06$) we achieved a steady state within 4000 time steps, which took about 6000 seconds with a Matlab code (running on a single CPU core), corresponding to 0.7 MLUPS. With Matlab running on the GPU we found about 1800 seconds, corresponding to 2.2 MLUPS.

It should be noted that the above results were obtained with codes that were not yet optimized with respect to calculation speed and memory performance. Currently we are working on the development of optimized codes in CUDA, both along the lines described in Ref. [13] (dedicated optimization) and by the generic optimization tools that will be developed in the project MACH. We expect to reach an enhancement of the calculation speed by at least one order of magnitude.

3 APPLICATION IN ACOUSTICS

3.1 Sound waves generated by a point source

The LB method can be used for simulating propagation of sound waves. We used the 2DQ9 LB model to model circular sound waves generated by a point source. Circular waves in 2D correspond to cylindrical waves in 3D. Figure 3 shows the sound field at time step 1600, generated by a point source at position (1000,1000) in a 2000x2000 grid with $\nu = 0.06$.

The fluid density at the source position was imposed at the end of each time step, according to the harmonic function $\rho = 1 + 0.01\sin(\omega t)$, where t is the time, $\omega = 2\pi / T$ is the angular frequency, and $T = 40$ is the harmonic period. The density oscillates around the equilibrium density of unity. The off-equilibrium density $\rho' \equiv \rho - 1$, or acoustic density, is given by (the real part) of the following function of time t and distance r to the source:

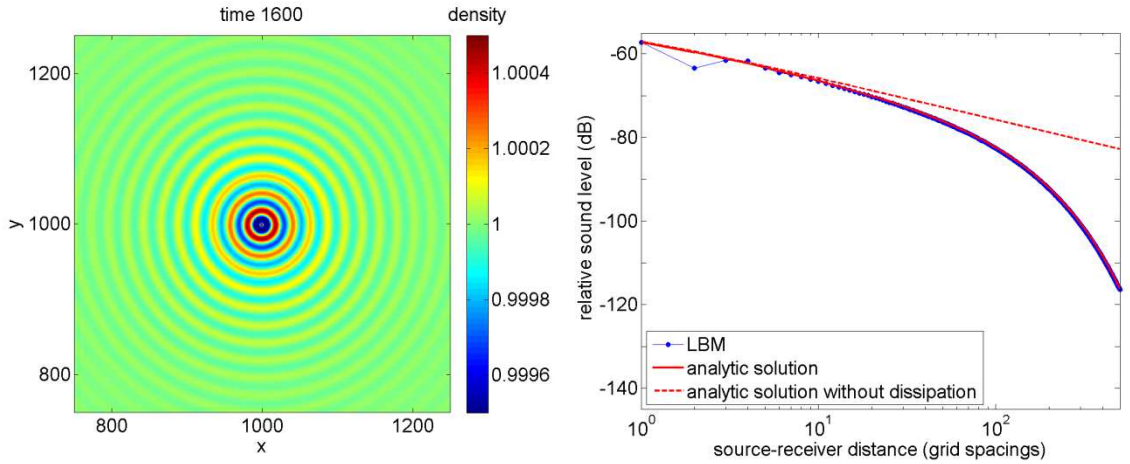

Figure 3: Results of a LB calculation for a sound wave, showing the sound field at time 1600 (left) and the relative sound level as a function of source-receiver distance (right).

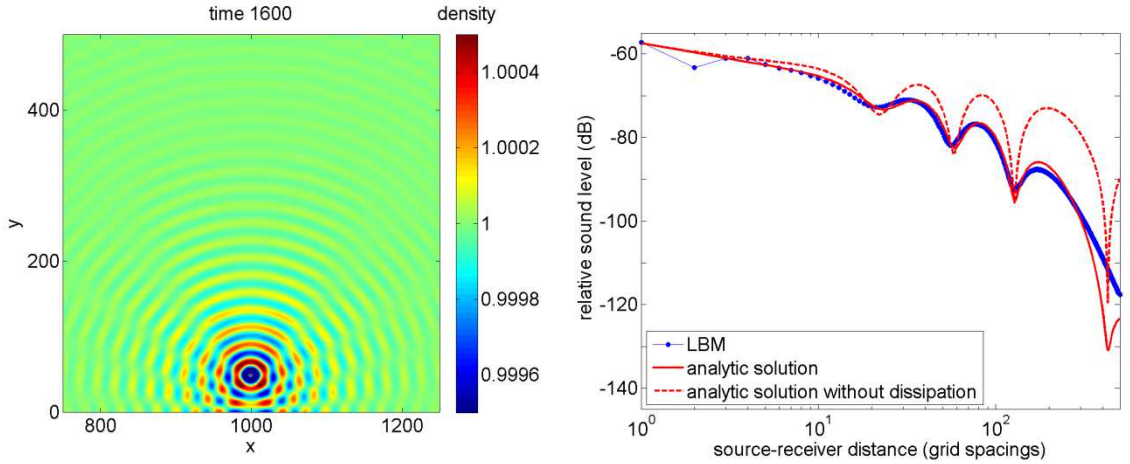

Figure 4: As Figure 3, for a point source and receivers at height $y = 50$.

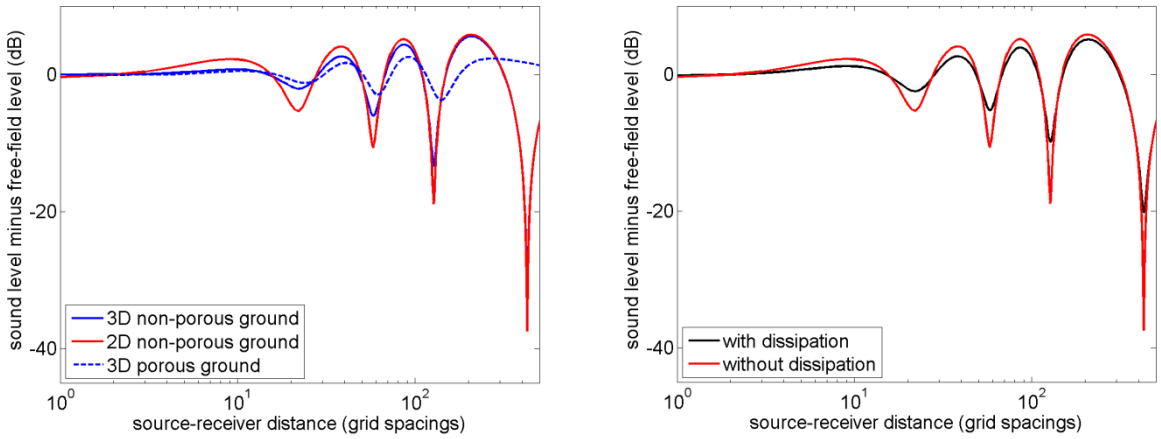

Figure 5: Analytical solutions for the sound level minus the free-field level, for the system of Figure 4 with a grid spacing of 0.1 m. The left graph shows 2D and 3D solution for non-porous and porous ground (without dissipation), and the right graph shows solutions with and without dissipation (2D, non-porous ground).

$$\rho' = AH_0^{(2)}(kr)\exp(i\omega t), \tag{3}$$

where A is a constant, $H_0^{(2)}$ is the Hankel function of order zero and second kind, and k is the wavenumber. This expression is a stationary solution of the lossy wave equation, taking into account effects of viscosity [6][18]. The wave number is given by $k = \omega/c_S - i\alpha_s$, where we have $\alpha_s = (\omega/\sqrt{2}c_s)\sqrt{[\sqrt{1+(\omega\tau_s)^2}-1]/[1+(\omega\tau_s)^2]}$ and $\tau_s = c_s^{-2}(\frac{4}{3}\nu+\nu')$, with kinematic shear and bulk viscosities ν and $\nu' = \frac{2}{3}\nu$. The wavelength is equal to $T\cdot c_S$, which is 23 lattice units in this case, in agreement with the wave pattern shown in Figure 3. The amplitude of the wave decreases with distance r from the source by two effects, geometrical spreading and dissipation. Geometrical spreading is represented by the factor $r^{-1/2}$, which is the asymptotic behavior of the Hankel function for real wavenumber k. Dissipation due to viscosity is represented by the imaginary part α_s of the wave number. Figure 3 shows how the relative sound level, defined as $20\lg\rho'_{\mathrm{rms}}$, with ρ'_{rms} the rms-value of ρ', decreases with distance r. The LBM results agree with the analytic solution beyond a distance of three grid spacings (blue dots and the red solid line coincide here). Also shown is the analytic solution without dissipation ($\alpha_s = 0$), which decays with 10 dB per distance decade ($20\lg 10^{-1/2} = -10$ dB). The figure demonstrates that dissipation dominates the attenuation at large distance, where the attenuation reaches a value of about 0.06 dB per grid spacing in this case.

The dissipation is a problem for direct application of the LB method in acoustics. The dissipation of sound waves in air is small, typically 0.1 dB/km at frequency 50 Hz and 1 dB/km at 250 Hz. If we choose a grid spacing of 0.1 m, for example, the above attenuation in the LB system is 0.6 dB/m, so much larger than real attenuations at audio frequencies. The attenuation in the LB system can be varied a bit through the choice of the value of $\nu = c_s^2(\tau - \frac{1}{2})$, but as indicated before numerical difficulties may occur for τ near $\frac{1}{2}$, so the possible variation is limited. A better approach may be to keep the frequency in the LB model low, thereby maximizing the region where geometrical attenuation dominates, and to convert the results to a real system by adding air absorption afterwards and applying the acoustical principle of scaling to convert to higher frequencies.

3.2 Effect of a non-porous ground surface

We have simulated the sound field of a point source near a non-porous ground surface. The system is similar to the previous system, except now we used a 2000x500 grid and the source was located at position (1000,50), so the source is 50 grid spacings above the ground surface. Figure 4 shows the results. The effect of interference between direct and reflected sound waves is visible as spatial oscillations of the sound level. The sound level was sampled at receivers at positions (1001-1500,50).

The analytic solutions in Figure 4 were calculated by (coherent) summation of the direct field and the field reflected by the ground surface. The LBM results agree well with the analytic solution (with dissipation). The analytic solutions are also represented in Figure 5,

now expressed as the excess level ΔL, defined as the sound level minus the free-field level. The dissipation effects largely cancel with this level difference. The LB units may be converted to physical units by assuming a grid spacing of 0.1 m, for example. This means that source and receivers are 5 m above the ground surface, and the frequency is 148 Hz.

Also included in Figure 5 is a 3D solution, calculated with $\exp(-ikr)/r$ instead of $H_0^{(2)}(kr)$. The difference in ΔL between the 2D solution and the 3D solution is small. The figure shows further that the dissipation effects largely cancel in the quantity ΔL. It is common practice in acoustics to work with excess level ΔL. The actual free field may be added to obtain the overall field.

The solution for a porous ground in Figure 5 deviates considerably from the other solutions, and is considered in the next section.

3.3 Effect of a porous ground surface

Next we have used the LB method for simulating the reflection of sound waves by a porous medium. We used a grid with 2000x700 nodes, with numerical parameters as before. The region between $y = 0$ and $y = 200$ was filled with a porous medium, and source and receivers were located at $y = 250$. The porous medium was generated by randomly selecting 30 percent of the nodes as solid nodes, where LB bounceback conditions apply. Figure 6 shows the results. The interference pattern is less pronounced than with the non-porous ground, since the reflection from the porous ground is weaker.

The analytic solution in Figure 6 was calculated with a theoretical model for sound reflection from a porous ground (see Ref. [8]), where we assumed again a grid spacing of 0.1 m to convert LB units to physical units. The total sound field is the sum of the direct field and the field reflected by the ground surface. The acoustic impedance of a porous ground is a function of the flow resistivity, the porosity, and a structure factor [19] (see also [8][9]). In this case, the porosity is 0.7, for the structure factor we used a value of 3, and the flow resistivity was estimated at 10 kPa s m^{-2} from a LB simulation illustrated in Figure 7. For this simulation we used a 100x100 grid with porous medium between $y = 25$ and $y = 75$, and an upward inflow condition at $y = 0$. The flow resistivity was estimated from the definition as the ratio of the pressure gradient and the velocity.

We also performed a calculation with the LB method for the same system as for Figure 6 with zero porosity, i.e. with a non-porous ground surface. The result should agree with the result shown in Figure 4, which was the case in good approximation. Small differences were attributed to small differences in the two LB implementations.

Figure 8 compares the results for porous and non-porous ground in terms of excess level ΔL. Both the LBM results and the analytic solutions show that the interference minima and maxima are more pronounced for the non-porous ground than for the porous ground. The differences between the LBM results and the analytic solutions should be investigated further. The approximations in both the LB method and the analytic solutions may play a role.

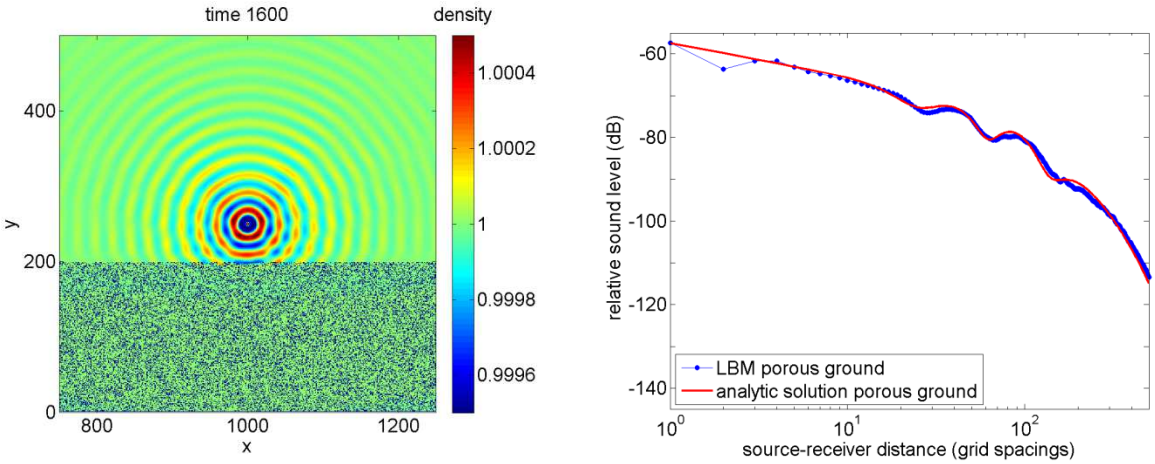

Figure 6: Results of a LB calculation for a point source and receivers at $y = 250$ and a porous medium below $y = 200$, showing the sound field at time 1600 (left) and the relative sound level as a function of distance (right).

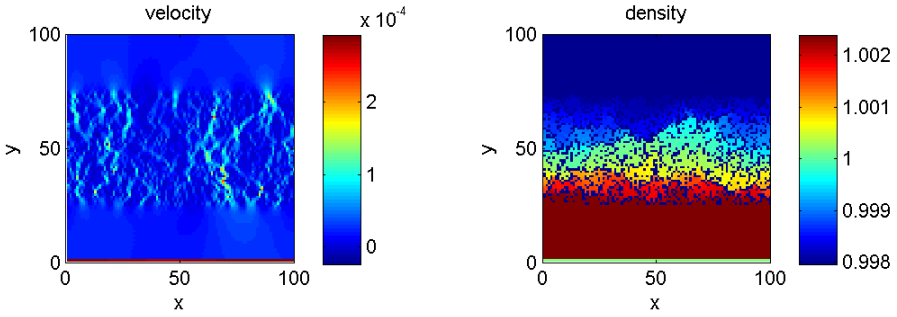

Figure 7: Stationary vertical velocity field (left) and density field (right) in a 100x100 LB system with a porous medium between y=25 and y=75 and an upward inflow condition at y=0, used for estimating the flow resistivity.

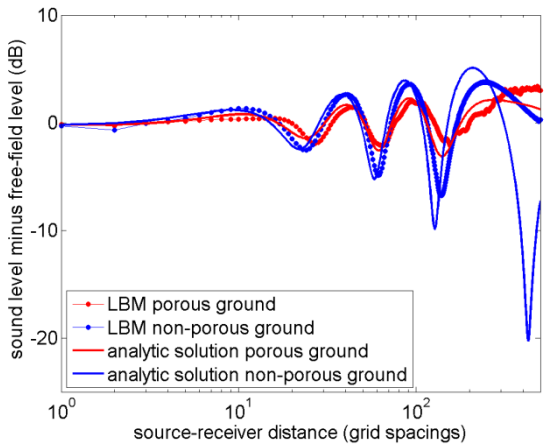

Figure 8: LB results and analytic solutions for porous and non-porous ground, expressed as the excess level ΔL as a function of distance.

3.4 Effect of a noise barrier

Finally we have used the LB method for simulating the effect of a noise barrier on a non-porous ground surface. We used a grid with 2000x1000 nodes, with numerical parameters as before. The source was located at position (1000,50). The noise barrier was located at position x = 1100, with a height of 100 grid spacings. Receivers were located at positions $x = 1001$ to $x = 1500$, at a height of $y = 50$. Figure 9 shows the results. The effect of the noise barrier is a decrease of the sound level by about 30 dB.

In Figure 10 the results are shown in terms of the excess level ΔL. Also included is an analytic solution for receivers behind the barrier, which deviates a bit from the LBM results. This solution is based on a theory of diffraction of spherical sound waves by wedge-shaped objects [20][21]. Dissipation was not included in the solution.

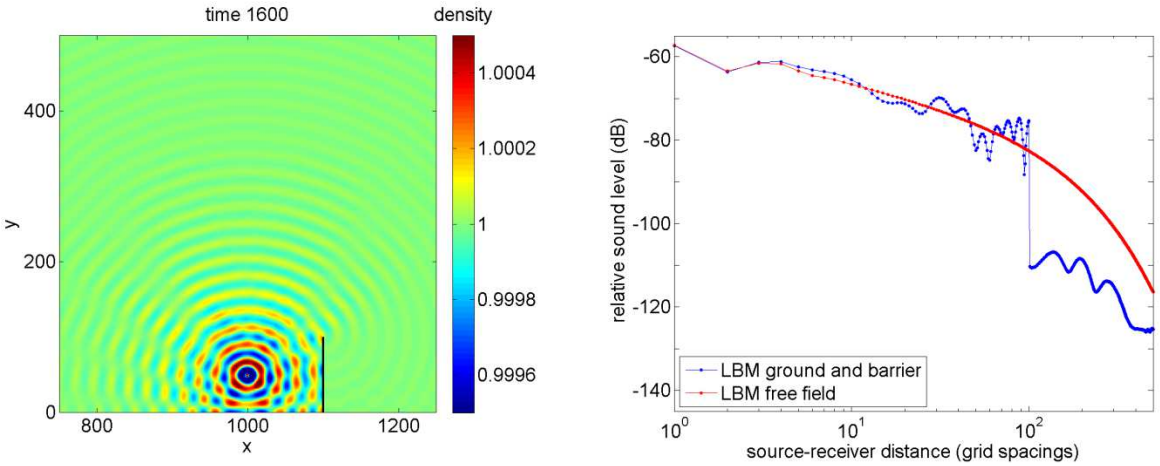

Figure 9: Results of a LB calculation for a non-porous ground surface with a noise barrier at $x = 1100$ (black line), showing the sound field at time 1600 (left) and the relative sound level as a function of distance (right).

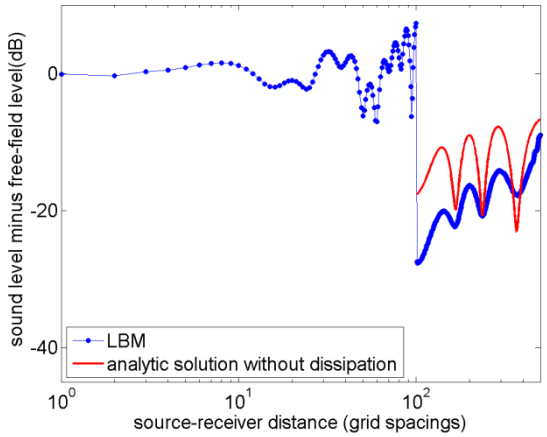

Figure 10: LBM result from Figure 9 and analytic solution, expressed as the excess level ΔL as a function of distance.

3.5 Refraction by wind and temperature gradients

The LB method can in principle deal with wind flow and sound propagation in a single simulation. This is an important advantage of the LB method over other sound propagation models. Wind effects on outdoor sound propagation are large, in particular in situations with noise barriers. The LB method may be extended to include temperature gradients [22], which also affect sound propagation.

4 CONCLUSIONS

In this paper we have explored application of the LB method in acoustics. LBM results were compared with analytic solutions for relatively simple cases, including cases with reflection by porous and non-porous ground surfaces and a case with screening and diffraction by a noise barrier. Reasonable agreement was obtained. The power of the LB method is that it can be applied to cases with complex boundary conditions, as illustrated here for the case with a porous ground surface. Another advantage of the LB method is that it can handle in principle wind flow and sound propagation in a single simulation.

A problem is the large dissipation of sound waves in an LBM simulation. Part of the dissipation effects are eliminated by considering the excess sound level, i.e. the level in excess of the free-field level. One may also keep dissipation effects small by choosing the sound frequency low and scale the results to higher frequencies. This will be explored in future work.

REFERENCES

[1] Reichl, L.E., *A Modern Course in Statistical Physics*, (Edward Arnold, London,1980), pp.468-475, 523-528.

[2] Hughes, W.F., and Brighton, J.A., *Fluid Dynamics*, Schaum's outline series, (McGraw-Hill, New York, 1967), pp. 1-47.

[3] Sukop, M.C., and Thorne Jr., D.T., *Lattice Boltzmann Modeling, An Introduction for Geoscientists and Engineers*, (Springer, Berlin, 2007).

[4] Latt, J., Chopard, B., Malaspinas, O., Deville, M., and Michler, A., "Straight velocity boundaries in the lattice Boltzmann method", *Phys. Rev. E* (2008) **77** 056703.

[5] Buick, J.M., Greated, C.A., and Campbell, D.M., "Lattice BGK simulations of sound waves", *Europhys. Lett.* (1998) **43**:235-240.

[6] Viggen, E.M., "The lattice Boltzmann method with applications in acoustics", thesis NTNU 2009, Norway.

[7] Viggen, E.M., "The lattice Boltzmann method: Fundamentals and acoustics", PhD thesis NTNU 2014, Norway.

[8] Salomons, E.M., *Computational atmospheric acoustics* (Kluwer, Dordrecht, 2001).

[9] Salomons, E.M., Blumrich, R., and Heimann, D., "Eulerian time-domain model for sound propagation over a finite-impedance ground surface. Comparison with frequency-domain models", *Acta Acustica united with Acustica* (2002) **88**: 483-492.

[10] Van Renterghem, T., and Botteldooren, D., "Prediction-step staggered-in-time fdtd: An efficient numerical scheme to solve the linearised equations of fluid dynamics in outdoor

sound propagation", *Appl. Acoust.* (2007) **68**: 201-216.
[11] Hornikx, M., Waxler, R., and Forssén, J., "The extended Fourier pseudospectral time-domain method for atmospheric sound propagation", *J. Acoust. Soc. Am.* (2010) **128**: 297-319.
[12] The MACH project is a European ITEA project. The project website is http://www.mach-project.org.
[13] Tölke, J., and Krafczyk, M., "TeraFLOP computing on a desktop PC with GPUs for 3D CFD", International Journal of Computational Fluid Dynamics (2008) **22**: 443 — 456.
[14] Feichtinger, C., "Design and performance evaluation of a software framework for multiphysics simulations on heterogeneous computers", PhD thesis (2012), Erlangen-Nürnberg University.
[15] Zou, Q., and He, X., "On pressure and velocity boundary conditions for the lattice Boltzmann BGK model", *Phys. Fluids* (1997), **9**: 1591-1598.
[16] For more information on CUDA, see http://www.nvidia.com
[17] Latt, J., "Choice of units in lattice Boltzmann simulations", April 2008, see http://wiki.palabos.org/howtos:main/.
[18] Kinsler, L., Frey, A., Coppens, A., and Sanders, J., *Fundamentals of Acoustics* (John Wiley & Sons, New York, 2000).
[19] Zwikker, C., and Kosten, C.W., *Sound absorbing Materials* (Elsevier, New York, 1949).
[20] Salomons, E.M., "Sound propagation in complex outdoor situations with a non-refracting atmosphere: model based on analytical solutions for diffraction and reflection", *Acta Acustica united with Acustica* (1997) **83**: 436-454.
[21] Hadden, J.W., and Pierce, A.D., "Sound diffraction around screens and wedges for arbitrary point source locations", *J. Acoust. Soc. Am.* (1981) **69**: 1266-1276.
[22] Guo, Z., Shi, B., and Zheng, C., "A coupled lattice BGK model for the Boussinesq equations", *Int. J. Numer. Meth. Fluids* (2002) **39**: 325-342.